MRS Communications (2017), 7, 152–165

doi:10.1557/mrc.2017.25

MRS Communications

Prospective Article

Nanostructured layered vanadium oxide as cathode for high-performance sodium-ion batteries: a perspective

Wen Luo, State Key Laboratory of Advanced Technology for Materials Synthesis and Processing, Wuhan University of Technology, Wuhan 430070, China; Laboratoire de Chimie et Physique: Approche Multi-échelles des Milieux Complexes, Institut Jean Barriol, Université de Lorraine, Metz 57070, France
Jean-Jacques Gaumet, Laboratoire de Chimie et Physique: Approche Multi-échelles des Milieux Complexes, Institut Jean Barriol, Université de Lorraine, Metz 57070, France
Liqiang Mai, State Key Laboratory of Advanced Technology for Materials Synthesis and Processing, Wuhan University of Technology, Wuhan 430070, China; Department of Chemistry, University of California, Berkeley, California 94720, USA

Address all correspondence to Jean-Jacques Gaumet at **jean-jacques.gaumet@univ-lorraine.fr** and Liqiang Mai at **mlq518@whut.edu.cn**

(Received 22 January 2017; accepted 7 April 2017)

Abstract

Sodium-ion batteries (SIBs) have received intensive attentions owing to the abundant and inexpensive sodium (Na) resource. Layered vanadium oxides are featured with various valence states and corresponding compounds, and through multi-electron reaction they are capable to deliver high Na storage capacity. The rational construction of unique structures is verified to improve their Na storage properties. This perspective provides an overview of recent advances in layered vanadium oxide for SIBs, with a particular focus on construction of novel nanostructures, and mechanism studies via in situ characterization. Finally, we predict possible breakthroughs and future trends that lie ahead for high-performance layered vanadium oxides SIBs cathode.

Introduction

Recently, there are increasing concerns of sustainable energy and environment due to the growing consumption of nonrenewable fossil fuels. The urgent requirement for clean and renewable energy sources has stimulated the rapid development of efficient, stable and reliable electricity supply systems. Lithium-ion batteries (LIBs) have been widely utilized in modern society such as in portable electronic device, electrical vehicles (EVs), and large-scale grid.[1–3] Recently, with the great concerns about the limited lithium (Li) resource, sodium-ion batteries (SIBs) have emerged as one of promising alternatives to LIBs due to its abundant and inexpensive sodium (Na) resource.[4,5] Meanwhile, Na has been studied to exhibit suitable redox potential and similar intercalation chemistry to Li; thus, SIBs hold promise to be viable complement or replacement to LIBs as the next-generation energy storage device.[6,7] However, the larger radius of Na^+ ions requires an expanding host space when a typical sodiation/desodiation process occurs. Consequently the size effect of Na^+ ions would result in severe damage on the lattice structure of the host. Besides, Na^+ ions are demonstrated to exhibit lower diffusion rate compared with Li^+ ions. Therefore, the understanding and development of reliable cathode with suitable lattice space to host Na^+ ions are the key issues to be addressed.

Vanadium oxides feature unique open-layered structures, which allow a diversity of other cations or molecules to insert into the layers.[8,9] In LIBs, these open-layered structures are capable to accommodate more Li^+ ions, thus give rise to higher specific capacity than those of the commercial cathodes.[10] Moreover, vanadium oxides display rich redox chemistry due to different oxidation states and coordination geometries, therefore resulting in their different valence states and phase structures. With concerns to their layered structures, vanadium oxides generally contain [VO_6] octahedral geometry with less [VO_4] tetrahedron. Basically, these octahedral can form two-dimensional (2D) sheet structures by sharing edges and/or corners (sometimes faces).[11] These octahedral or tetrahedron possessed with a long V–O bond (2.1–2.6 Å, and 2.79 Å in V_2O_5 itself) and a short vanadyl bond, –V = O (1.55–1.75 Å) are capable to form various layered structures (Fig. 1). As depicted in literature, a double chain of edge-sharing [VO_6] octahedral is the basic assembly unit. When the double chains are congregated by sharing the side corners, and a single layer can occur in most vanadium oxides [Fig. 1(a)]. In orthorhombic α-V_2O_5 [Fig. 1(b)], a short vanadyl bond and the other longer V–O bonds coexist. Consequently, the vanadium coordination polyhedron changes into a square pyramid due to the longer weak bond [weak V–O bond illustrated in Fig. 1(c)].[11] As suggested by Sohn et al., when these $(V_2O_4)_n$ chains closely aligned by sharing edges, no-vacancy square-pyramidal layered VO_2 is formed [Fig. 1(f)].[12] V_6O_{13} structure is formed by single and double layers sharing corners alternatively [Fig. 1(e)].[13] When all the apices (vanadyl bonds) emerge up in one layer and also down in the other layers, a typical double

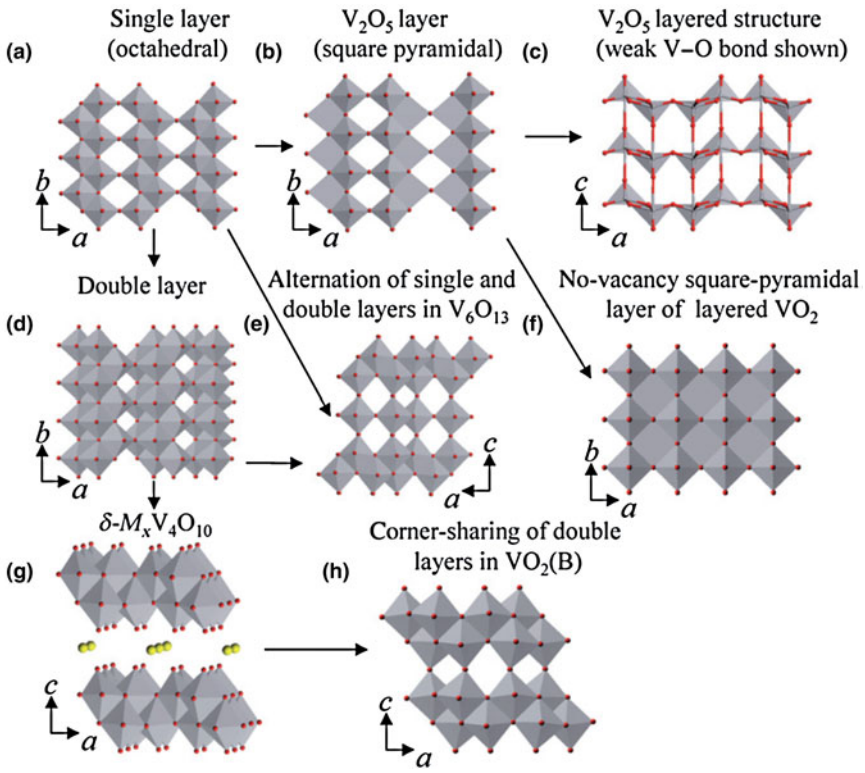

Figure 1. Various layered vanadium oxide structures: (a) single layer of V_2O_5 (octahedral); (b) single layer of V_2O_5 (square pyramid); (c) layer structure of α-V_2O_5; (d) double layer of V_2O_5; (e) alternation single and double layer of V_6O_{13}; (f) no-vacancy square pyramidal layer of VO_2; (g) structure of δ-$M_xV_4O_{10}$; (h) corner sharing stacking of double layers in VO_2(B). (Adapted/reproduced with permission from Ref. 11, Royal Society of Chemistry, 2009.)

layer of δ-type vanadium oxides can be created from single sheets [Fig. 1(g)]. To avoid confusion with double-sheet V_2O_5, this unique double layer of vanadium oxide is designated as δ-$M_xV_4O_{10}$, which predominately exists in most of vanadium oxides gels.[14] When double layers of the δ-$M_xV_4O_{10}$ structure collapse through the elimination of the interlayer species such as water molecule or metal ions, a metastable form of vanadium dioxide VO_2(B) is constructed [Fig. 1(h)].[15]

The sodiation/desodiation in vanadium oxide cathode are complex multi-electronic reaction processes. The applications of vanadium oxides in SIBs are restricted by rapid capacity fading caused by a decrease of the Na diffusion coefficient and severe structure deterioration. The concept of enhancing Na storage performance via nanostructuring has been recognized in numerous research works.[16–20] These novel nanostructures are proved to possess robust structural integrity and stability, faster electrochemical reaction rate, and enhanced reaction reversibility. In this perspective, we provide a brief review of recent advances in several typical vanadium oxides, and discussions on the engineering of unique nanostructures and its beneficial effects on enhancing the SIBs performance. Some intriguing and insightful studies of in situ X-ray diffraction (XRD) characterization on vanadium oxides for SIBs will be provided. Finally, perspective outlooks will be carefully addressed based on recent advances on the construction and understanding of nanostructured layered vanadium oxide for high-performance SIBs cathode.

Electrochemical performance of layered vanadium oxide cathode for SIBs

Binary vanadium oxide

In general, large families of vanadium oxides include binary vanadium oxides (containing V and O elements exclusively) and multicomponent vanadium oxides. Firstly, we briefly provided representative recent advances of the layered binary vanadium oxides cathode systems, together with their electrochemical cycling data for SIBs, as summarized in Table. 1.

VO_2

VO_2 have been reported to exist in dozens of different phases species with their particular structural characteristics.[21,22] Among these known phases, metastable VO_2(B) exhibits layered structure to allow the intercalation of guest ions for high-performance SIBs. Various novel VO_2(B) nanostructures have been reported, such as VO_2(B) nanospheres,[23] nanowires,[24] nanosheets,[25] nanowires assembled hollow spheres,[26] and micro/nano-structured nanoparticles.[27] It should be noted that, in a typical heat treatment or solution reaction process, VO_2(B) trends to transform into monoclinic phase VO_2(M)

Table 1. Summary of representative recent advances of the binary layered vanadium oxides (containing V and O elements exclusively) cathode systems, together with their electrochemical cycling data for SIBs.

Compound	Reversible capacity	Cycling performance	Main advances	Ref
Single-crystalline VO_2 nanosheets	179 mA h/g at 20 mA/g	Capacity remains at 108 mA h/g over 50 cycles at the current density of 500 mA/g	The reaction during charge/discharge can happen between $Na_{0.3}VO_2$ and $NaVO_2$	[28]
Graphene quantum dots coated VO_2 arrays	306 mA h/g at 100 mA/g	A capacity of more than 110 mA h/g after 1500 cycles at 18 A/g	A binder-free cathode by bottom-up growth of biface VO_2 arrays directly on a graphene network was achieved	[29]
Carbon quantum dots coated VO_2 nanowires	328 mA h/g at 0.3 C	A capacity of 133 mA h/g even at the rate of 60 C	The energy and power densities of as-fabricated cathode for Na storage reach 264 Wh/kg and 41333 W/kg	[30]
VO_2/rGO nanorods	160 mA h/g at 60 mA/g	The capacity retention is 90% after 400 cycles (against 2th) at 1 C	Phase amorphization of VO_2 (B) occurs when potential below 0.5 V	[31]
α-V_2O_5/C composite	183 mA h/g at 40 mA/g	A capacity over 90 mA h/g at a high current density of 640 mA/g	A large portion of Na-ion storage at high rates is due to V_2O_5 pseudocapacitance	[20]
α-V_2O_5 hollow nanospheres	159 mA h/g at 20 mA/g	A capacity of 109.5 mA h/g after 100 cycles at 160 mA/g	The exposed {110} crystal planes of V_2O_5 with 2D diffusion path Na^+ contribute to excellent performance	[33]
α-V_2O_5/C composite	192 mA h/g at a current density of 0.05 C	A capacity of 160 mA h/g at 1 C	The reversible change of oxidation state of vanadium was verified as $V^{4+}\leftrightarrow V^{5+}$ (de/sodiation)	[32]
Bilayered porous V_2O_5 nanoribbons	250 mA h/g at 20 mA/g	85% of its initial value up to 350 cycles under various current rates	An electrochemically responsive bilayered structure with adjustable interlayer spacing was evidenced to accommodate Na^+ intercalation	[34]
Bilayered sponge-like V_2O_5 nanosheets	216 mA h/g at 20 mA/g	Capacity retention of 73% for 100 cycles at a current density of 100 mA/g	The thin nanosheets along [001]-axis provide short diffusion pathways for Na ions	[36]
Bilayered V_2O_5 nanobelts	231.4 mA h/g at 90 mA/g	170 mA h/g after 100 cycles at current density of 80 mA/g	Exposed {100} crystal planes provide large interlayer spacing (~11.53 Å) for Na^+ intercalation	[35]
$V_2O_5{\cdot}2.1H_2O$	130 mA h/g at 560 mA/g	325, 250, and 150 mA h/g at C/10, 1 C, and 7 C, respectively	Green binder system was used to optimize Na^+ intercalation	[41]
$V_2O_5{\cdot}0.55H_2O$	A high initial capacity of 338 mA h/g at 0.05 A/g	High-rate capacity of 96 mA h/g at 1 A/g	Pseudocapacitive behavior makes a great contribution to the high capacities	[42]
Fe-VO_x nanobelts	An initial capacity of 184 mA h/g at 0.1 A/g	High-rate capacities of 118 and 92 mA h/g obtained at 1.0 and 2.0 A/g	Iron pre-intercalation to reduce the lattice expansion/contraction upon cycling	[43]
Amorphous V_2O_5	175 mA h/g at a current density of 23.6 mA/g	Overall charging–discharging rates are much faster, a capacity of 78 mA h/g at a current density of 1180 mA/g	The fast Faradaic reactions occur in amorphous V_2O_5	[52]
Amorphous V_2O_5 particles	265 mA h/g at a current density of 80 mA/g	Both amorphous and crystalline V_2O_5 cathodes can be reversibly worked for 10,000 cycles at 2560 mA/g.	Amorphous V_2O_5 cathode possesses higher reversible capacities than the crystalline V_2O_5 at low current densities, whereas it is inversed at high current densities	[53]

and tetragonal phase VO_2(R), which barely exhibit electrochemical activity. Therefore, the controllable synthesis of pure phase VO_2(B) is critical for its good electrochemical performance. Jiao and co-workers for the first time synthesized single-crystalline VO_2(B) parallel ultrathin nanosheets for the cathode material in SIBs via a simple hydrothermal method.[28] As the number of the inserted Na^+ ions increases from 0 to 1.0, the formation energy gets lower, implying the formation of the more stable phase. As the number of inserted Na^+ ions excess 1.0, the formation energy of Na_xVO_2 becomes more positive compared with $NaVO_2$, and on this occasion, the discharge process cannot take place spontaneously [Fig. 2(a)]. As they indicated that when the number of inserted Na^+ ions per formula increases from 0.25 to 1, the interlayer distance changes a little. For more Na ions inserted into the tunnels ($x > 1$), the cell volume begins to expand consecutively. The backbone of the V–O tunnels is completely broken down and the stability and reversibility of the VO_2-like structure are destroyed [Fig. 2(b)]. The proposed reaction mechanism can be illustrated as $VO_2 + xNa^+ + xe^- \leftrightarrow Na_xVO_2$ [Fig. 2(c)] based on their findings.

The weak Na^+ ions transport kinetics has been considered as the major drawback of cathode electrode for SIBs. Nanoscale surface engineering has significant effects on promoting the reaction kinetic of battery electrode. Chao et al. reported a binder-free cathode composed of VO_2 arrays directly growing on graphene networks for SIBs cathode [Figs. 3(a)–3(f)].[29] The integrated electrode delivers a capacity of 306 mA h/g at 100 mA/g, and a capacity of more than 110 mA h/g after 1500 cycles at 18 A/g [Fig. 3(g)]. Furthermore, at the ultrahigh rate of 120 C, the power density based on mass of the whole electrode is as high as 42 kW/kg with an energy density of more than 100 W h/kg [Fig. 3(h)]. Tong and co-workers also reported an unique free-standing cathode consisted of carbon quantum dots coated VO_2 nanowires.[30] The carbon quantum dots, which are flexible for surface engineering can efficiently ensure the integrity of nanowire. Another interesting work demonstrates the facile microwave-assisted solvothermal method to fabricate VO_2(B)/ reduced graphene oxide (rGO) with good Na storage performance.[31] The phase amorphization of VO_2 when potential bellows 0.5 V confirmed some stable metal oxides might display better behavior in SIBs than expected.

Orthorhombic V_2O_5

With respect to orthorhombic V_2O_5, a storage mechanism was proposed by Chung and co-workers that the appearance of NaV_2O_5 was a major phase with minor $Na_2V_2O_5$ when fully discharged.[32] Their synchrotron based near edge X-ray adsorption fine structure (NEXAFS) spectroscopy results also suggested the charge compensation during desodiation/sodiation process accomplished by the reversible changes between $V^{4+} \leftrightarrow V^{5+}$. As for the Na storage performance of α-V_2O_5 cathode, the major issue hinders the performance caused by the slow Na ion diffusion. Therefore, the controllable synthesis of α-V_2O_5 electrode materials with versatile nanostructures plays an important role for achieving good electrochemical performance. Ji and co-workers reported an orthorhombic V_2O_5 coated inside nanoporous carbon composite for SIBs cathode. For the first time they demonstrated that this composite displays superior Na storage performance [Figs. 4(a) and 4(b)],[20] and a capacity of over 90 mA h/g at a current rate of 640 mA/g [Fig. 4(c)]. They also demonstrated V_2O_5 pseudocapacitance contributes to a large portion of the Na storage especially under high current rates operating condition [Figs. 4(d) and 4(e)].

Void architecture and exposed crystal planes of V_2O_5 nanocrystals have been confirmed to enhance good high-rate capability and cycling stability of α-V_2O_5. Wang and co-workers synthesized hollow orthorhombic V_2O_5 hierarchical nanospheres through a polyol-induced template-free solvothermal approach [Fig. 4(f)].[33] Transmission electron microscopy (TEM) [Fig. 4(g)] and refined XRD analyses [Fig. 4(h)] revealed that the V_2O_5 hollow nanospheres were composed of hierarchical nanocrystals and most of these nanocrystals exhibit exposed {110} crystal planes. V_2O_5 hollow nanosphere shows a high initial discharge capacity of 223 mA h/g; however, only 159 mA h/g discharge capacity is obtained after the second cycle. The achieved capacity is equal to the intercalation of one Na ion for each formula unit to form a crystal structure of NaV_2O_5 [Fig. 4(i)].

Bilayered V_2O_5

Bilayered V_2O_5 has attracted much interest due to its larger interlayer distance compared to that of aforementioned α-V_2O_5. Rajh and co-workers found that bilayered V_2O_5 stacks are split up by large interlayer spacing, which is evidenced by as a broad strong peak at high d spacing (~13.5 Å), confirmed by X-ray scattering [Figs. 5(a) and 5(b)] and TEM results [Figs. 5(c)–(e)].[34] Notably, bilayered V_2O_5 undergoes an entirely different intercalation mechanism compared to orthorhombic V_2O_5. Two phase transitions have been discovered when Na^+ ions incorporate into the orthorhombic electrode, implying that the orthorhombic crystalline structure changes two times to accommodate increased concentration Na^+ ions. In contrast, no phase transitions occur when Na^+ ions intercalate into bilayered V_2O_5, revealed by the representative smooth, solid state solution intercalation profiles [Fig. 5(f)]. Notably, the crystallinity of the materials does not degenerate during cycling and the sample maintains stable crystalline structure after 80 cycles [Fig. 5(g), red curve]. In a word, the intercalation of Na^+ ions causes arrangement of structure to possess both long- and short-range order; whereas the deintercalation process results in the loss of long-range order and the retention of short-range order [Fig. 5(h)].

Besides, more articles also reported high-performance bilayered V_2O_5 cathode for SIBs with controllable nanostructures, such as single-crystalline bilayered V_2O_5 nanobelts,[35] sponge-like layered V_2O_5 nanosheets.[36] A large (001) interlayer spacing (~11.53 Å) of V_2O_5 nanobelts can accommodate Na-ion intercalation and deintercalation. Interestingly, the unique bilayered vanadium oxide nanobelts were revealed to possess

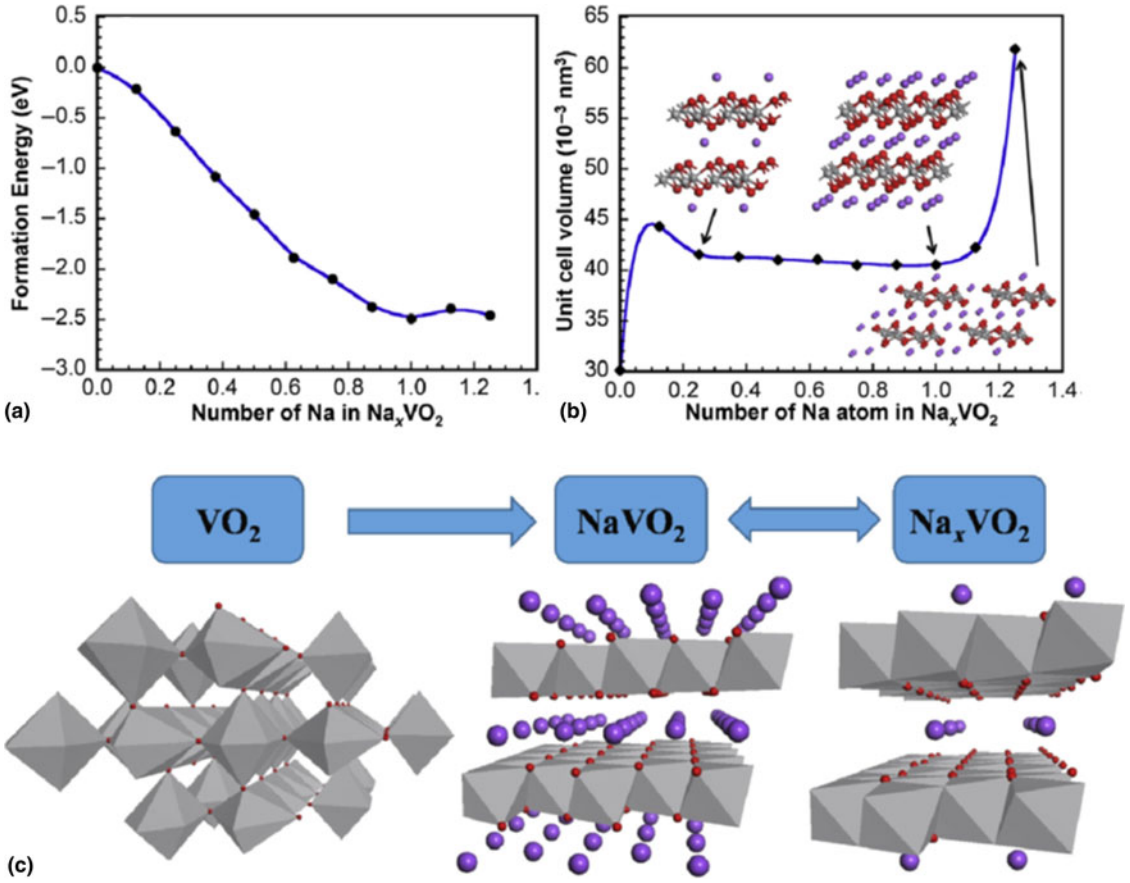

Figure 2. (a) The relationship between the formation energy and the number of Na ions in Na_xVO_2. (b) Volume with respect to the number of Na ions in a VO_2 molecule. (c) Schematic illustration of Na ions insertion and extraction process. (Adapted/reproduced with permission from Ref. 28, Elsevier, 2014.)

predominantly exposed {100} crystal planes, which offer large interlayer spacing for facile Na extraction/insertion.[35]

$V_2O_5{\cdot}nH_2O$

The reduced structural order, the large interlayer space and the short diffusion length are the key factors that allow $V_2O_5{\cdot}nH_2O$ to reversibly host cations.[37,38] Recently, Moretti and Passerini provided a comprehensive review on bilayered nanostructured $V_2O_5{\cdot}nH_2O$ for metal batteries, which confirms the renewed interests on $V_2O_5{\cdot}nH_2O$ for energy storage.[39] Briefly, $V_2O_5{\cdot}nH_2O$ can be obtained in xerogel or aerogel depending on different drying methods. This unique $V_2O_5{\cdot}nH_2O$ is a representative class of δ-$M_xV_4O_{10}$ [Fig. 1(g)] where water molecules intercalate and regular the layer spacing.[40]

A variety of methods to prepare $V_2O_5{\cdot}nH_2O$ as thin film or bulk powder have been developed. Among them, vapor deposition (physical or chemical) and solution methods draw great interests due to their facility and versatility. For example, Passerini and co-workers employed supercritical fluid (CO_2) extraction to eliminate the water in V_2O_5 and fabricate a porous aerogel $V_2O_5{\cdot}nH_2O$ ($n = 2.1$) [Fig. 6(a)].[41] When applied as a SIBs cathode, high specific capacities were achieved due to its open framework with expanded interlayer spacing and decreased diffusion path [Fig. 6(b)]. Mai and co-workers developed a facile freeze-drying process to synthesize a $V_2O_5{\cdot}nH_2O$ xerogel composed of thin interconnected nanowire networks [Fig. 6(c)].[42] Ex situ XRD indicated the layer of $V_2O_5{\cdot}nH_2O$ is shrinking/expanding accompanied by the Na^+ ion insertion/extraction, which is different from the irreversible phase transition of α-V_2O_5 [Figs. 6(d) and 6(e)]. Ex situ Fourier transform infrared spectroscopy (FTIR) results demonstrated that the crystal water is not completely replaced during Na^+ ion insertion [Fig. 6(f)]. To improve its stability, iron preintercalated vanadium oxide ultrathin nanobelts (Fe-VO_x) with constricted interlayer spacing were fabricated.[43] The electrochemical performances of $V_2O_5{\cdot}nH_2O$ have been enhanced via electrolyte optimization[44] or cut-off voltage,[45] even though long-term cycling stability still need to be addressed.

Amorphous V_2O_5

Amorphous electrode materials have received considerable interests as they can reduce the stress and might provide isotropic transport path for ions compared with crystalline materials.[9,46]

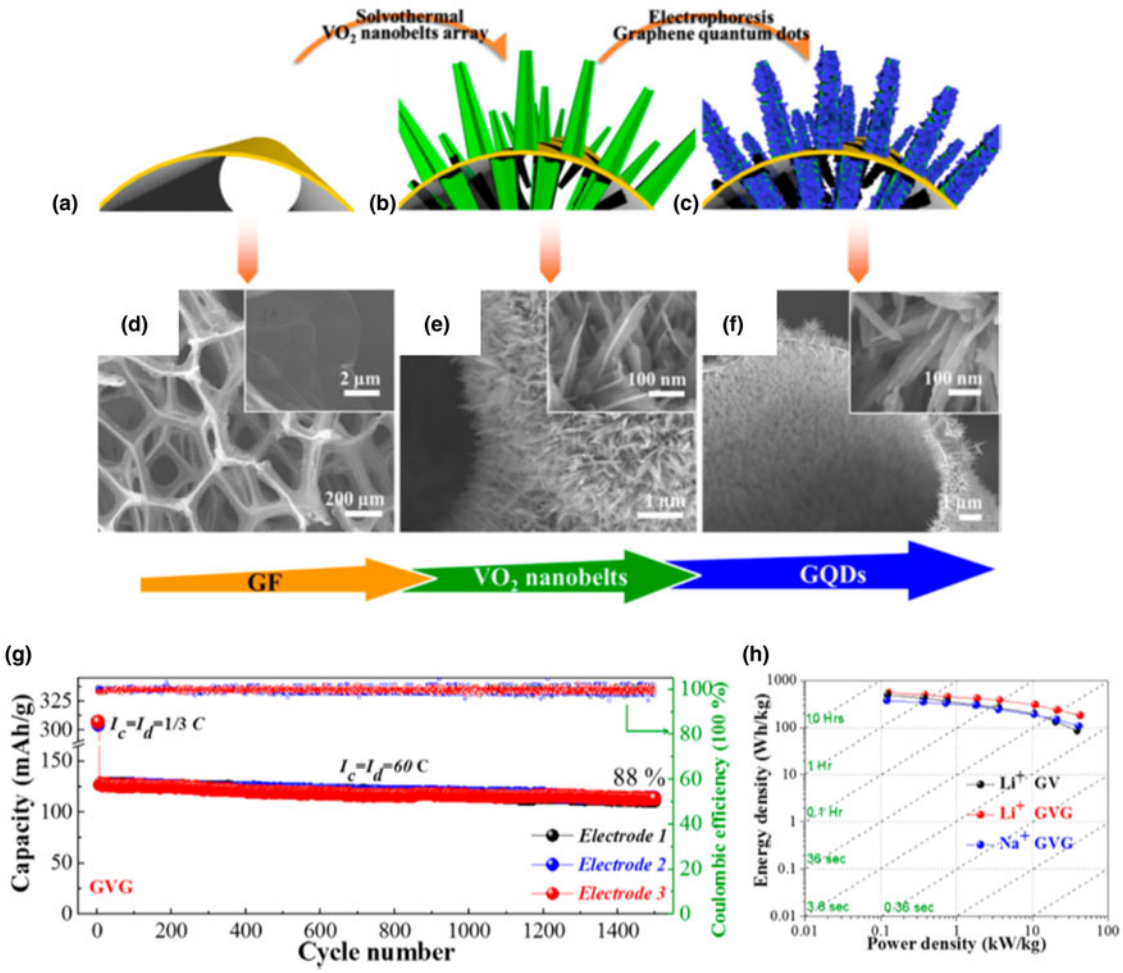

Figure 3. (a–c) Fabrication process of GF supported GQDs-coated VO_2 nanobelts array, (d–f) the corresponding SEM images in each process, respectively. (g) Cycling performance of the three electrodes at 60 C for 1500 cycles (1/3 C at the first five cycles for activation); (h) Ragone plot based on the total mass of the whole electrode, the sloping lines indicate the relative time to get the charge in or out of the electrodes. (Adapted/Reproduced with permission from Ref. 29, American Chemical Society, 2015.)

As exemplified in some reports, some amorphous aerogels or xerogel prepared are featured with low density, highly porous and high surface area and are being explored as new promising materials in electrochemistry.[47–51] Gao et al. demonstrated amorphous V_2O_5 exhibited superior Na storage performance compared with its crystalline counterpart.[52] No distinctive peak can be observed when the cyclic voltammetry (CV) scan was conducted on this amorphous V_2O_5, however the current response was scaled with the potential and was even greater than that of the crystalline counterpart. The less ordered and abundant open channels decrease the diffusion barrier for Na^+ ions to transport, which contribute to high-rate capability and high-energy density. The amorphous matrix makes it easier for Na^+ ions to intercalate into the crystal and diffuse deeper into the host material. Due to the isotropic penetration pathway of ions rather than some certain preferential directions, the overall charging–discharging rates are much faster, as evidenced by a capacity of 78 mA h/g at a current density of 1180 mA/g. Recently, Li and co-workers demonstrated that amorphous V_2O_5 cathode possesses higher reversible capacities than the crystalline V_2O_5 at low-current densities, whereas it is inversed at high current densities.[53] Therefore, the rational selection of amorphous or crystalline V_2O_5 cathode for SIBs need to be further investigated with respects to various operation requirements.

Layered-structured vanadate compounds

Layered-structured vanadates are studied as typical layered vanadium oxides incorporating second metals such as Li, Na, or transition metals such as cobalt, silver, and iron. In this short perspective article, we will focus on the classic intensively studied $Na_3V_2(PO_4)_3$ (NVP) composites and emerged promising $K_3V_2(PO_4)_3$ composites in this group and get inspiration upon the investigation of other vanadate compounds.

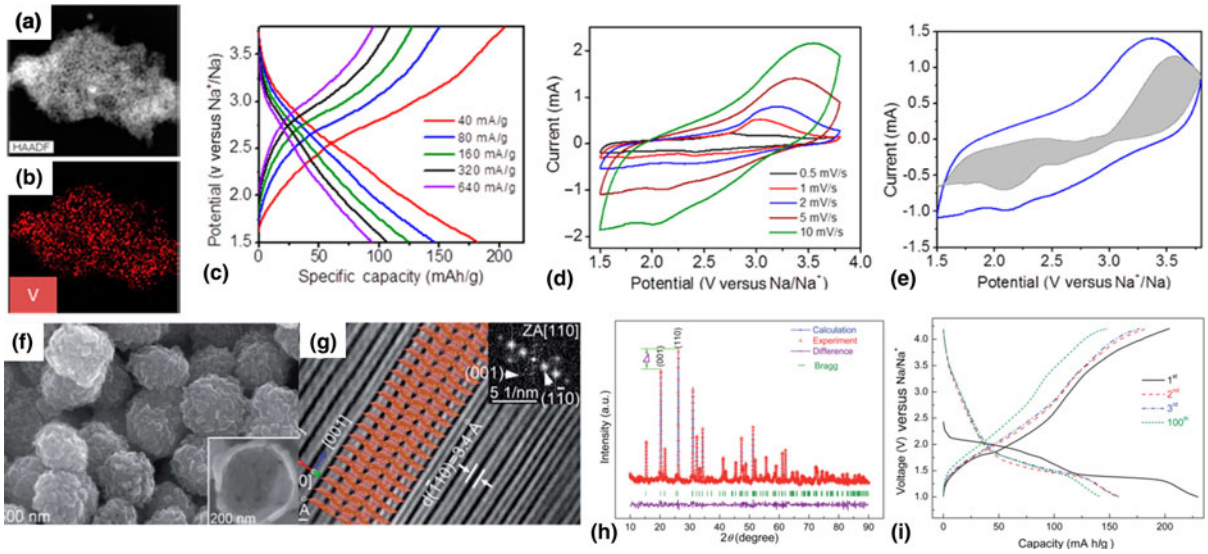

Figure 4. (a) HAADF-STEM image of V_2O_5-nanoporous carbon (RFC) and the corresponding EDX mappings of (b) vanadium; (c) Galvanostatic charge–discharge profiles of 55-V_2O_5-RFC at various current densities. (d) CV profiles of 55-V_2O_5-RFC at different scanning rates from 0.5 to 10 mV/s. (b–e) CV profile for 55-V_2O_5-RFC at a sweeping rate of 5 mV/s. The estimated capacitive current contribution is shown in the shaded region. (Adapted/Reproduced with permission from Ref. 20, American Chemical Society, 2014.) (f) FESEM image of V_2O_5 nanospheres. (g) FFT pattern along the (110) zone axis of V_2O_5 and inset in the middle of (g) is the simulated V_2O_5 (110) crystal plane. (h) Rietveld refinement pattern of XRD data for V_2O_5 nanospheres. The observed and calculated intensities are represented by red crosses and the blue solid line, respectively. (i) 1st, 2nd, 3rd, and 100th cycle discharge and charge profiles of V_2O_5 hollow nanospheres at 20 mA/g current density. (Adapted/reproduced with permission from Ref. 33, Royal Society of Chemistry, 2014.)

$Na_3V_2(PO_4)_3$

Among the big family of vanadium compounds, NVP have been intensively studied as SIBs cathodes because of its high theoretical capacity and stable Na super ion conductor (NASICON) structure.[54–59] Especially, NVP displays two potential plateaus located at 3.4 and 1.6 V versus Na/Na^+, related to the V^{3+}/V^{4+} and V^{2+}/V^{3+} redox couples, respectively.[55] These two reactions can provide a specific capacity of approximately 117 and 50 mA h/g at the high- and low-voltage zones, respectively. Since the first report on superior electrochemical performance and storage mechanism of NVP cathode for room-temperature SIBs,[16] numerous literatures demonstrated the great advances in performance enhancement and mechanism investigation, which cannot be totally included in this perspective. Herein some great advances are exemplified subsequently. Carbon or graphene modification has been proven as an efficient strategy to improve conductivity and rate capability. A hierarchical carbon framework wrapped NVP composite is fabricated via chemical vapor deposition on NVP particles.[60] The NVP hybrid electrode can exhibit a high reversible capacity of 115 mA h/g at 0.2 C and long-term cycling stability (a capacity retention of 54% after 20,000 cycles). Mai and co-workers designed a novel synthesis of layer-by-layer NVP@ rGO nanocomposite by adjusting the surface charge of NVP gel precursor [Fig. 7(a)].[61] The NVP@rGO nanocomposite contains trace amount of rGO and amorphous carbon, yet displays superior electrochemical performance [Fig. 7(b)]. The morphological optimization of NVP material has a great significance for improving the electrochemical performance since NVP suffers from intrinsic low electronic conductivity. For this purpose, Mai and co-workers introduced a novel 3D NVP nanofiber network controllably constructed via a facile self-sacrificed template method.[62] The as-synthesized material displays excellent cyclability (95.9% capacity retention over 1000 cycles at 10 C) and enhanced high-rate performance (94 mA h/g at 100 C) for Na half-cell. Notably, when evaluated as full battery [$NaTi_2(PO_4)_3$ as anode] cathode, it also shows outstanding cycling stability (96.9% capacity retention over 300 cycles at 5 C) and superior rate capability (80 mA h/g at 50 C). Such remarkable performance is attributed to the 3D nanofiber network structure, which provides multi-channel ionic diffusion pathway, continuous electronic conduction, and improved structural integrity.

$K_3V_2(PO_4)_3$

Apart from intensively researched Na vanadates, a new type of potassium phosphate material $K_3V_2(PO_4)_3$, was designed for the first time and explored for Na storage by Mai et al.[63] $K_3V_2(PO_4)_3$/C bundled nanowires were fabricated through a simple organic acid-assisted approach [Figs. 7(c) and 7(d)]. Beneficial from a stable framework, nanoporous structure, and conductive carbon coating, the $K_3V_2(PO_4)_3$/C bundled nanowires cathode displays good electrochemical performances in SIBs. A capacity of 119 mA h/g can be achieved at a current density of 100 mA/g and $K_3V_2(PO_4)_3$/C bundled

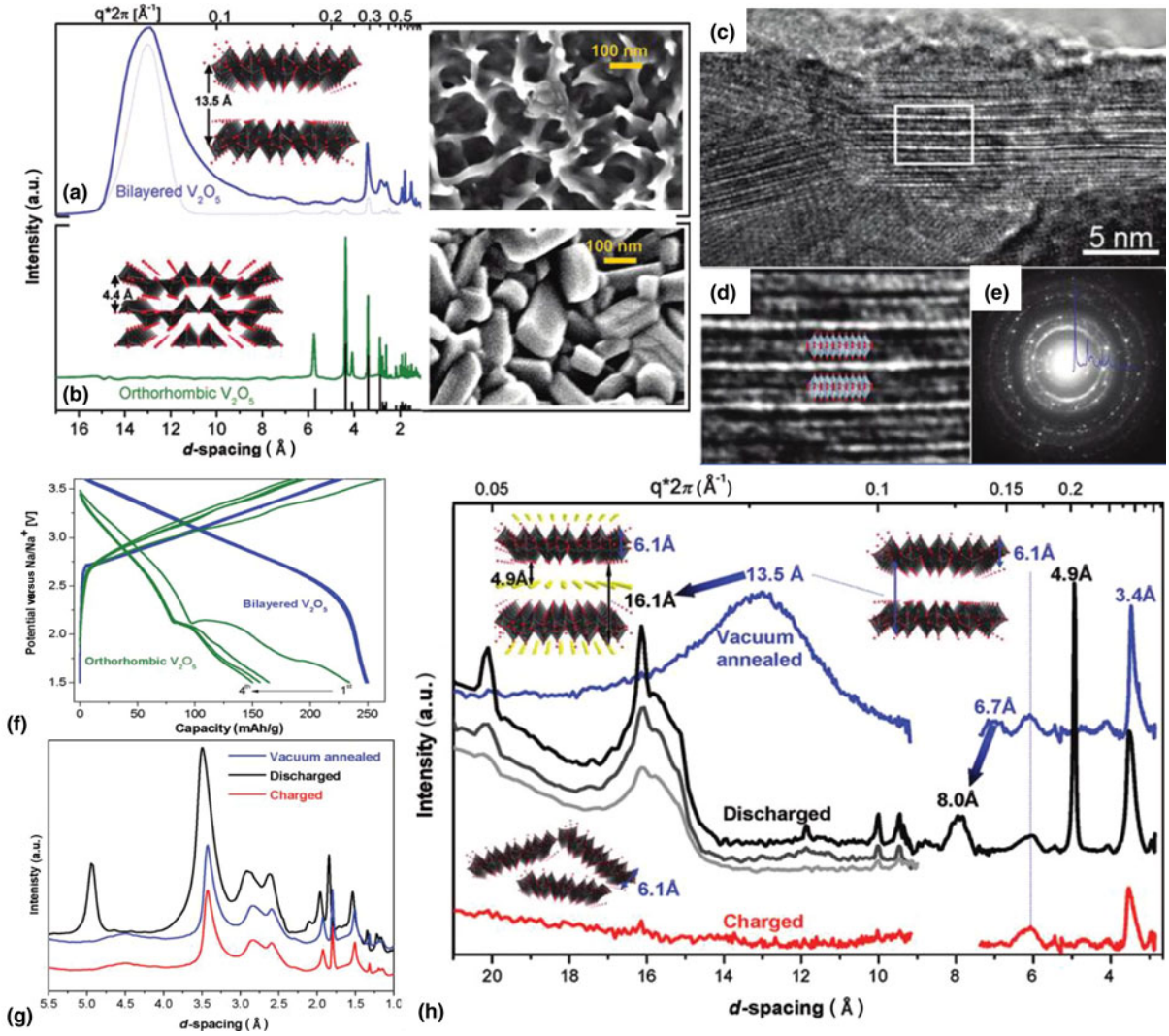

Figure 5. XRD patterns, SEM images and the molecular simulations based on the monoclinic bipyramid layer structure model of (a) bilayered and (b) orthorhombic V_2O_5; (c, d) HRTEM images, and (e) SAED pattern of bilayered-V_2O_5; (f) Charge and discharge curves of first four cycles of bilayered-V_2O_5 and α-V_2O_5 electrodes at the current density of 20 mA/g; (g) Synchrotron XRD spectra of bilayered V_2O_5 annealed in vacuum at 120 °C (blue), in discharge after Na^+ ion intercalation (black) and in charged state after Na^+ ion deintercalation (red). (h) SAXS and WAXS spectra for bilayered V_2O_5 for as-deposited, in discharge and charged state. (Adapted/reproduced with permission from Ref. 34, American Chemical Society, 2012.)

nanowires exhibit enhanced electrochemical performance compared to bulk KVP at various current densities [Fig. 7(e)].

In situ characterization of layered vanadium oxide cathode

In situ characterization has been recognized as a powerful tool to provide deeper and more direct insights into the materials degradation and phase transformation mechanisms under real-time working condition.[64–66] The comprehensive understanding of morphological and microstructural changes of layered vanadium oxide cathode during charge and discharge processes are essential for the improving of the electrochemical performance.[67,68] Some advances on in situ XRD characterization of vanadium oxide cathode will be discussed to emphasize its importance and arouse broad research interests. For more knowledge on in situ characterization on energy storage materials, readers can be referred to some specific reviews.[64]

Delmas and co-workers firstly present the detailed phase diagram and in situ XRD experiments of the layered P2-Na_xVO_2 system for electrochemical Na insertion/extraction in SIBs.[69] Notably, four predominate single phase can be detected within the $0.5 \leq x \leq 0.9$ range [Figs. 8(a) and 8(b)]. During the Na insertion/extraction, they exhibit different Na/vacancy ordering between the VO_2 layers, which results in comparable or unmatched superstructures. Na^+ ions are found to perfectly order to minimize Na^+/Na^+ electrostatic repulsions [Fig. 8(c)]. Within the VO_2 layers, the vanadium ions tend to form pseudo-trimers possessing extremely short V–V distances

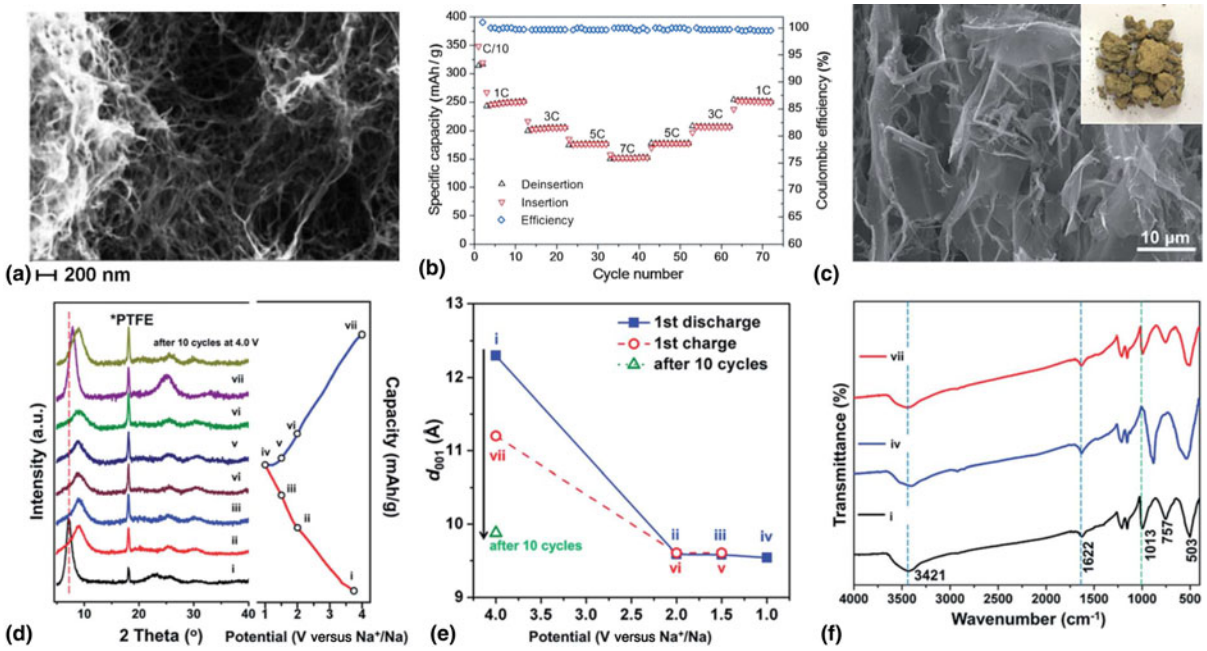

Figure 6. (a) SEM image of dried V_2O_5 powder; (b) Cycling behavior of V_2O_5 electrodes at high current densities. (Adapted/reproduced with permission from Ref. 41, Wiley, 2015.) (c) SEM image of $V_2O_5{\cdot}nH_2O$ xerogel. (d) Ex situ XRD patterns (e) related d_{001} value changes. (f) FTIR spectra of the $V_2O_5{\cdot}nH_2O$ xerogel cathodes in the SIB. (Adapted/Reproduced with permission from Ref. 42, Journal of Materials Chemistry A, Royal Society of Chemistry, 2015.)

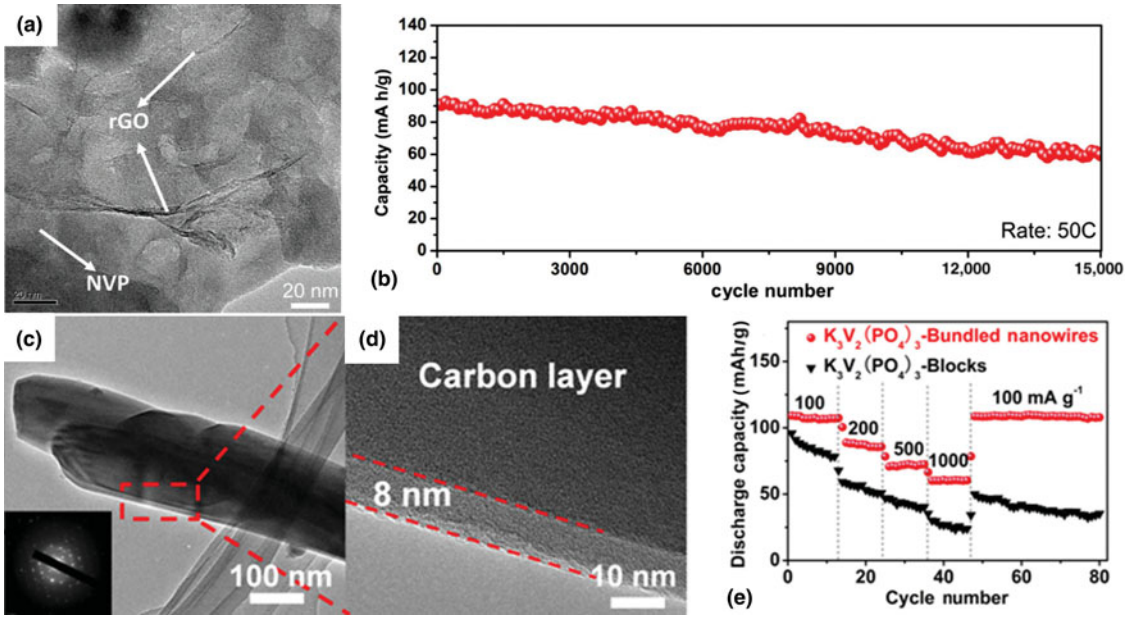

Figure 7. (a) TEM image of $Na_3V_2(PO_4)_3$@rGO; (b) ultraong cycling stability of the $Na_3V_2(PO_4)_3$@rGO for 15,000 cycles at a high rate of 50 C. (Adapted/reproduced with permission from Ref. 61, Wiley, 2016.) (c, d) HRTEM images of the $K_3V_2(PO_4)_3$/C bundled nanowires; (e) rate performance of the $K_3V_2(PO_4)_3$/C bundled nanowires and blocks. (Adapted/reproduced with permission from Ref. 63, Wiley, 2015.)

(two at 2.581 Å and one at 2.687 Å) [Figs. 8(d) and 8(e)]. More importantly, this phase exhibits a first-order structural transition beyond room temperature along with noticeable electronic and magnetic transitions. This work for the first time gets a precise study of phase diagram of this system in SIBs at room temperature, associated with in situ XRD experiments, and highlights the importance and powerfulness of in situ characterization combined with suitable simulation techniques.

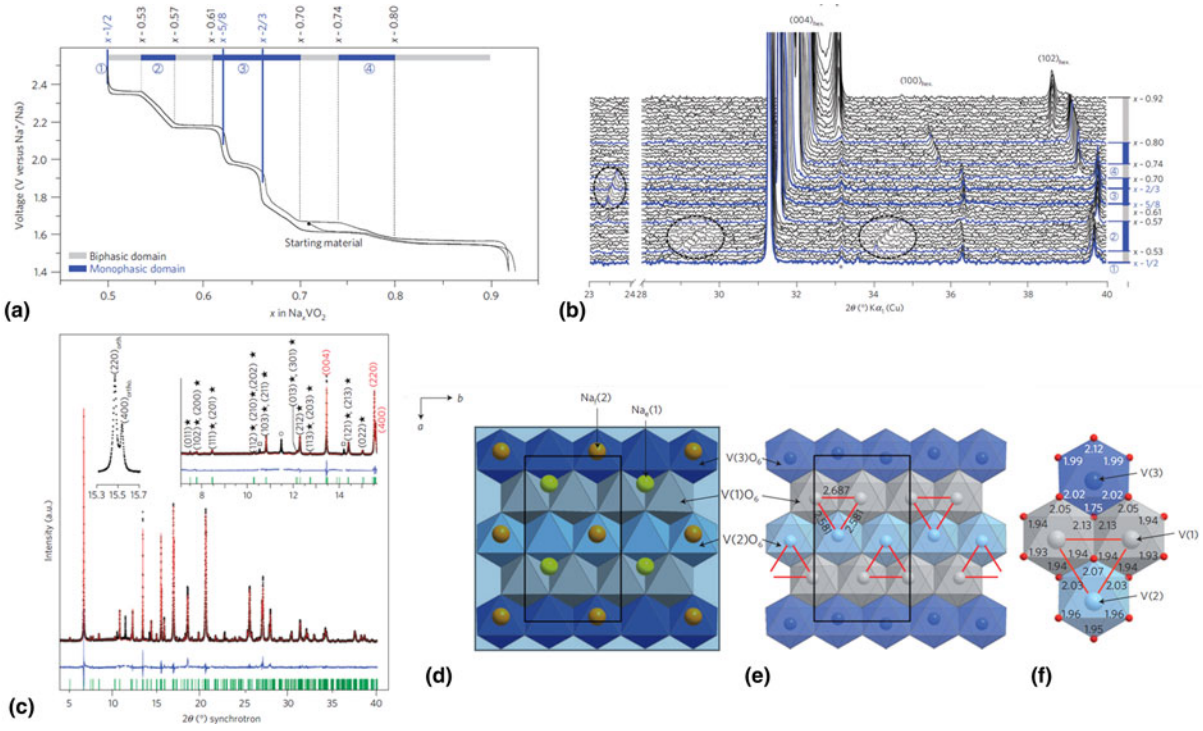

Figure 8. (a) Evolution of cell voltage as a function of Na content in Na_xVO_2 over the $0.5 \leq x \leq 0.92$ range; (b) In situ XRD data recorded during the galvanostatic intermittent titration technique experiments. (c) Synchrotron diffraction pattern of P2-$Na_{1/2}VO_2$ and Rietveld refinement of its structure. (d–f) Projection of the structure of P2-$Na_{1/2}VO_2$ along the *c*-axis. (Adapted/reproduced with permission from Ref. 69, Nature Publishing Group, 2012.)

In situ XRD characterization can also provide detailed structure information for new-type vanadium oxide cathode candidates for SIBs. Mai et al. employed a new-type $K_3V_2(PO_4)_3$/C as cathode materials for SIBs.[63] Through in situ XRD investigation, the intensity and position of peak shifted during the charge and discharge reversibly, corresponding to the (de)insertion of K^+/Na^+ and the expansion/extraction of the lattice distance [Figs. 9(a) and 9(b)]. The vanadium phosphate showed excellent stability, which allows the deinsertion of K^+ ion and insertion of Na^+ ion without collapse of crystal structure.

Beside, in situ XRD characterizations are capable to offer direct observation on crystal structure evolution of cathode material during Na^+ ions insertion/deinsertion process. The prepared NVP nanofiber in situ cell was charged to 3.9 V and then discharged to 2.3 V. All the $Na_{3-\alpha}V_2(PO_4)_3$ peaks disappear on charge and are restored on discharge; Conversely, $Na_\beta V_2(PO_4)_3$ peaks start to form and grow on charge and disappear on discharge [Figs. 9(d) and 9(e)].[62] It is clear that the (211) and (300) peaks shift to higher angles during charge process, indicating that the *d*-spacings decrease during the Na^+ ions de-insertion. After recharging to 3.9 V, the peaks return to the original positions, indicating the good reversibility.

Summary and outlook

As discussed above, notable progress has been made on the synthesis of vanadium oxide for high-performance SIBs along with some in situ XRD characterizations to disclose its intrinsic Na storage mechanism. However, there are still big challenges to be faced. Some perspectives are carefully addressed here, and the future studies on vanadium oxide as SIBs cathode are suggested to be deliberately initiated in the following aspects:

(1) Developing facile, efficient, sustainable, and controllable synthesis of novel nanostructures. In terms of the controllable synthesis of vanadium oxide cathode for SIBs, nanoscience engineering makes it possible to control the morphology and composition of cathode to effectively enhance the electrochemical performance. Recently, numerous reported method can be applied to obtain diverse nanostructures (i.e., hollow structure,[33] hierarchical heterostructures,[18,19,60] complex 3D architectures,[62] etc.) with peculiar electrochemical properties, interlayer spaces and morphologies. However, some synthetic methods are generally time-consuming and danger-risking in which various sophisticated steps and/or toxic, expensive chemicals involve. At this stage, developing facile, efficient and controllable synthesis of novel vanadium nanostructures is still urgently demanded. Therefore, more efforts shall be addressed on the knowledge and capability to construct the desired nanostructure architectures based on a comprehensive understanding.

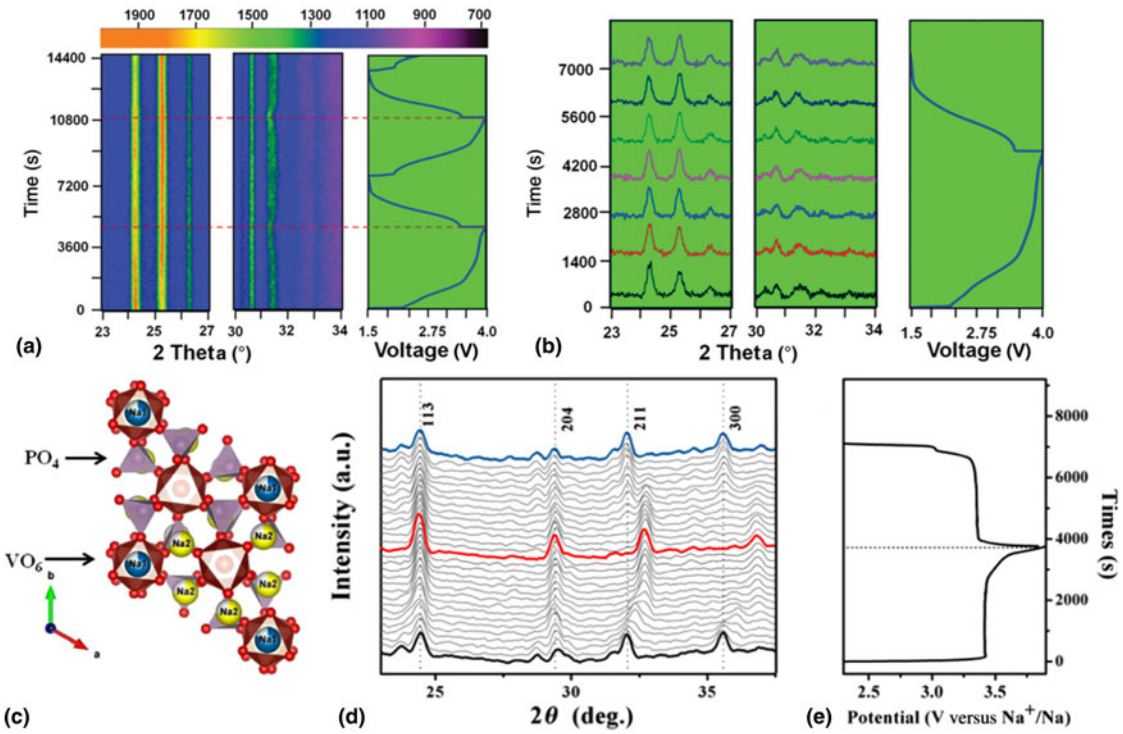

Figure 9. (a) The image plot of the diffraction patterns at 23–27° and 30–34° during the first two charge–discharge cycles of $K_3V_2(PO_4)_3$/C bundled nanowires. (b) Selected diffraction patterns during the first cycle stacked against the voltage profile. (Adapted/reproduced with permission from Ref. 63, Wiley, 2015.) (c) Crystal structure of $Na_3V_2(PO_4)_3$ (NVP); (d) The in situ XRD patterns of NVP for a full charge–discharge cycle; (e) The corresponding time–potential curve. (Adapted/reproduced with permission from Ref. 62, Elsevier, 2016.)

(2) Precisely designing and regulating layered structure with direct evidences. Normally, vanadium oxides feature rich redox chemistry due to different oxidation states and coordination geometries. The open framework facilitates ion movement, while the nanostructuring strategy can decrease the solid-state diffusion limitations and thus enhance the intercalation kinetics.[70] To name a few, preferentially exposed facets,[33,35] metal ions, or water molecule preintercalation[42,43] and the regulation of short-range order in layered structure[34] show great interests upon high-performance vanadium layered oxides. Whereas how to accurately tune the lattice space and stabilize its layered structure for long-term cycle needs to be addressed. Moreover, intercalation chemistry opens up a possibility to explore potential new-type vanadium oxide host materials for SIBs, and challenges and breakthroughs might lie ahead bearing the deeper understanding of solid state physics.

(3) Gaining insights into mechanism via various modern techniques. With regards to in situ characterization of cathode for SIBs, the working mechanisms of novel vanadium oxide cathode and their designing principles need further investigations. More direct evidences showing the correlation between the structure of the vanadium oxide and the electrochemical performance are greatly needed. For instance, although in situ XRD characterization show great advantages in observing the structural evolution of some typical vanadium oxides and present the detailed phase diagram, some important characterization methods (e.g., atomic force microscopy) are absent. Recent advances in the disclosing the role of structural H_2O in intercalation vanadium oxide are assisted by PDF (pair distribution function) analysis and/or DFT (density functional theory) calculations.[71] Intrinsic electrochemical mechanisms are expected to be addressed with the help of more advanced characterization instruments.[72–74] The combination of novel nanostructure design and computational simulation may be a feasible way.

(4) Better understanding of amorphous layered vanadium oxides. Notably, some amorphous vanadium oxides are demonstrated to exhibit impressive Na storage performance. Such outstanding electrochemical performance can be attributed to the large amounts of disordered lattice vacancies as well as abundant defects within the amorphous materials.[75] It has been studied the introduction of defect favors the development of optimized intercalation compounds and leads to substantial improvements for energy storage applications.[76] Nevertheless, to monitor the lattice vacancy and defect as well as disclose the possible effects on electrochemical performance still remains as a big

challenge. In an attempt to explore high-performance amorphous vanadium oxides for SIBs, new techniques and practical applications should be developed supported by numerous experimental and simulation results toward defects chemistry.

(5) Systematic and overall evaluation of the SIBs performance. Standardized methods for accurately characterizing the performance of full SIBs need to be established. Apparently, SIBs are indeed sophisticated systems associated with electrode structure, efficient electrolyte, packaging technology, and so forth. Comparing to the commercial LIBs, the development of high-efficiency electrolyte and separator, which are also vital for constructing high-performance vanadium oxide cathode-based full batteries, is insufficient. Currently, most reported research works on electrode materials have to conduct and present the optimization of electrolyte experiment for overall high-performance SIBs.[77–79] Besides, the rational choice of high-efficient binder and separator also highly depends on surface and interface chemistry knowledge.[80,81] Thus, to establish reliable standard system is essential for the development of commercial SIBs. Na-ion related knowledge must be deeply explored to introduce new alternative energy storage systems in the near future. Opportunities exist for researchers to bring together chemistry, physics, and engineering in imaginative morphologies.

Acknowledgment

This work was supported by the National Key Research and Development Program of China (2016YFA0202603), the National Basic Research Program of China (2013CB934103), the Programme of Introducing Talents of Discipline to Universities (B17034), the National Natural Science Foundation of China (51521001), the National Natural Science Fund for Distinguished Young Scholars (51425204), and the Fundamental Research Funds for the Central Universities (WUT: 2016-JL-004, 2016III001 and 2017III009). Prof. Dr. Liqiang Mai gratefully acknowledged financial support from China Scholarship Council (Grant no. 201606955096).

References

1. M. Armand and J.M. Tarascon: Building better batteries. *Nature* **451**, 652 (2008).
2. J.B. Goodenough and K.S. Park: The Li-ion rechargeable battery: a perspective. *J. Am. Chem. Soc.* **135**, 1167 (2013).
3. L. Mai, X. Tian, X. Xu, L. Chang, and L. Xu: Nanowire electrodes for electrochemical energy storage devices. *Chem. Rev.* **114**, 11828 (2014).
4. M.D. Slater, D. Kim, E. Lee, and C.S. Johnson: Sodium-ion batteries. *Adv. Funct. Mater.* **23**, 947 (2013).
5. V. Palomares, P. Serras, I. Villaluenga, K.B. Hueso, J. Carretero-González, and T. Rojo: Na-ion batteries, recent advances and present challenges to become low cost energy storage systems. *Energy Environ. Sci.* **5**, 5884 (2012).
6. S.W. Kim, D.H. Seo, X. Ma, G. Ceder, and K. Kang: Electrode materials for rechargeable sodium-ion batteries: potential alternatives to current lithium-ion batteries. *Adv. Energy Mater.* **2**, 710 (2012).
7. S.P. Ong, V.L. Chevrier, G. Hautier, A. Jain, C. Moore, S. Kim, X. Ma, and G. Ceder: Voltage, stability and diffusion barrier differences between sodium-ion and lithium-ion intercalation materials. *Energy Environ. Sci.* **4**, 3680 (2011).
8. L. Mai, X. Xu, L. Xu, C. Han, and Y. Luo: Vanadium oxide nanowires for Li-ion batteries. *J. Mater. Res.* **26**, 2175 (2011).
9. Q. An, F. Lv, Q. Liu, C. Han, K. Zhao, J. Sheng, Q. Wei, M. Yan, and L. Mai: Amorphous vanadium oxide matrixes supporting hierarchical porous Fe_3O_4/graphene nanowires as a high-rate lithium storage anode. *Nano Lett.* **14**, 6250 (2014).
10. D. Murphy, P. Christian, F. DiSalvo, and J. Waszczak: Lithium incorporation by vanadium pentoxide. *Inorg. Chem.* **18**, 2800 (1979).
11. N.A. Chernova, M. Roppolo, A.C. Dillon, and M.S. Whittingham: Layered vanadium and molybdenum oxides: batteries and electrochromics. *J. Mater. Chem.* **19**, 2526 (2009).
12. J.I. Sohn, H.J. Joo, D. Ahn, H.H. Lee, A.E. Porter, K. Kim, D.J. Kang, and M.E. Welland: Surface-stress-induced Mott transition and nature of associated spatial phase transition in single crystalline VO_2 nanowires. *Nano Lett.* **9**, 3392 (2009).
13. K.A. Wilhelmi, K. Waltersson, and L. Kihlborg: A refinement of the crystal structure of V_6O_{13}. *Acta Chem. Scand.* **25**, 2675 (1971).
14. P.Y. Zavalij and M.S. Whittingham: Structural chemistry of vanadium oxides with open frameworks. *Acta Crystallogr. B* **55**, 627 (1999).
15. Y. Oka, T. Yao, N. Yamamoto, Y. Ueda and A. Hayashi: Phase transition and V^{4+}-V^{4+} pairing in VO_2(B). *J. Solid State Chem.* **105**, 271 (1993).
16. Z. Jian, W. Han, X. Lu, H. Yang, Y.S. Hu, J. Zhou, Z. Zhou, J. Li, W. Chen, D. Chen, and L. Chen: Superior electrochemical performance and storage mechanism of $Na_3V_2(PO_4)_3$ cathode for room-temperature sodium-ion batteries. *Adv. Energy Mater.* **3**, 156 (2013).
17. S. Li, Y. Dong, L. Xu, X. Xu, L. He, and L. Mai: Effect of carbon matrix dimensions on the electrochemical properties of $Na_3V_2(PO_4)_3$ nanograins for high-performance symmetric sodium-ion batteries. *Adv. Mater.* **26**, 3545 (2014).
18. Y. Dong, S. Li, K. Zhao, C. Han, W. Chen, B. Wang, L. Wang, B. Xu, Q. Wei, and L. Zhang: Hierarchical zigzag $Na_{1.25}V_3O_8$ nanowires with topotactically encoded superior performance for sodium-ion battery cathodes. *Energy Environ. Sci.* **8**, 1267 (2015).
19. Q. Wang, B. Zhao, S. Zhang, X. Gao, and C. Deng: Superior sodium intercalation of honeycomb-structured hierarchical porous $Na_3V_2(PO_4)_3$/C microballs prepared by a facile one-pot synthesis. *J. Mater. Chem. A* **3**, 7732 (2015).
20. V. Raju, J. Rains, C. Gates, W. Luo, X. Wang, W.F. Stickle, G.D. Stucky, and X. Ji: Superior cathode of sodium-ion batteries: orthorhombic V_2O_5 nanoparticles generated in nanoporous carbon by ambient hydrolysis deposition. *Nano Lett.* **14**, 4119 (2014).
21. L. Mai, Q. Wei, Q. An, X. Tian, Y. Zhao, X. Xu, L. Xu, L. Chang, and Q. Zhang: Nanoscroll buffered hybrid nanostructural VO_2(B) cathodes for high-rate and long-life lithium storage. *Adv. Mater.* **25**, 2969 (2013).
22. E. Baudrin, G. Sudant, D. Larcher, B. Dunn, and J.M. Tarascon: Preparation of nanotextured VO_2(B) from vanadium oxide aerogels. *Chem. Mater.* **18**, 4369 (2006).
23. R. Li and C.Y. Liu: VO_2(B) nanospheres: hydrothermal synthesis and electrochemical properties. *Mater. Res. Bull.* **45**, 688 (2010).
24. L. Zhang, K. Zhao, W. Xu, J. Meng, L. He, Q. An, X. Xu, Y. Luo, T. Zhao, and L. Mai: Mesoporous VO_2 nanowires with excellent cycling stability and enhanced rate capability for lithium batteries. *RSC Adv.* **4**, 33332 (2014).
25. C. Nethravathi, C.R. Rajamathi, M. Rajamathi, U.K. Gautam, X. Wang, D. Golberg, and Y. Bando: N-doped graphene–VO_2(B) nanosheet-built 3D flower hybrid for lithium ion battery. *ACS Appl. Mater. Interface* **5**, 2708 (2013).
26. C. Niu, J. Meng, C. Han, K. Zhao, M. Yan, and L. Mai: VO_2 nanowires assembled into hollow microspheres for high-rate and long-life lithium batteries. *Nano Lett.* **14**, 2873 (2014).
27. E. Uchaker, M. Gu, N. Zhou, Y. Li, C. Wang and G. Cao: Enhanced intercalation dynamics and stability of engineered micro/nano-structured electrode materials: vanadium oxide mesocrystals. *Small* **9**, 3880 (2013).
28. W. Wang, B. Jiang, L. Hu, Z. Lin, J. Hou, and S. Jiao: Single crystalline VO_2 nanosheets: a cathode material for sodium-ion batteries with high rate cycling performance. *J. Power Sources* **250**, 181 (2014).

29. D. Chao, C. Zhu, X. Xia, J. Liu, X. Zhang, J. Wang, P. Liang, J. Lin, H. Zhang, and Z.X. Shen: Graphene quantum dots coated VO_2 arrays for highly durable electrodes for Li and Na ion batteries. *Nano Lett.* **15**, 565 (2015).
30. M.S. Balogun, Y. Luo, F. Lyu, F. Wang, H. Yang, H. Li, C. Liang, M. Huang, Y. Huang, and Y. Tong: Carbon quantum dot surface-engineered VO_2 interwoven nanowires: a flexible cathode material for lithium and sodium ion batteries. *ACS Appl. Mater. Interface* **8**, 15 (2016).
31. G. He, L. Li, and A. Manthiram: VO_2/rGO nanorods as a potential anode for sodium-and lithium-ion batteries. *J. Mater. Chem. A* **3**, 28 (2015).
32. G. Ali, J.H. Lee, S.H. Oh, B.W. Cho, K.W. Nam, and K.Y. Chung: Investigation of the Na intercalation mechanism into nanosized V_2O_5/C composite cathode material for Na-ion batteries. *ACS Appl. Mater. Interface* **8**, 9 (2016).
33. D. Su, S. Dou, and G. Wang: Hierarchical orthorhombic V_2O_5 hollow nanospheres as high performance cathode materials for sodium-ion batteries. *J. Mater. Chem. A* **2**, 11185 (2014).
34. S. Tepavcevic, H. Xiong, V.R. Stamenkovic, X. Zuo, M. Balasubramanian, V.B. Prakapenka, C.S. Johnson, and T. Rajh: Nanostructured bilayered vanadium oxide electrodes for rechargeable sodium-ion batteries. *ACS Nano* **6**, 530 (2012).
35. D. Su and G. Wang: Single-crystalline bilayered V_2O_5 nanobelts for high-capacity sodium-ion batteries. *ACS Nano* **7**, 11218 (2013).
36. K. Zhu, C. Zhang, S. Guo, H. Yu, K. Liao, G. Chen, Y. Wei, and H. Zhou: Sponge-like cathode material self-assembled from two-dimensional V_2O_5 nanosheets for sodium-ion batteries. *ChemElectroChem* **2**, 1660 (2015).
37. D. McNulty, D.N. Buckley, and C. O'Dwyer: Synthesis and electrochemical properties of vanadium oxide materials and structures as Li-ion battery positive electrodes. *J. Power Sources* **267**, 831 (2014).
38. M. Giorgetti, S. Passerini, W.H. Smyrl, and M. Berrettoni: Evidence of bilayer structure in V_2O_5 xerogel. *Inorg. Chem.* **39**, 1514 (2000).
39. A. Moretti and S. Passerini: Bilayered nanostructured V_2O_5·nH2O for metal batteries. *Adv. Energy Mater.* (2016). DOI: 10.1002/aenm.201600868.
40. V. Petkov, P.N. Trikalitis, E.S. Bozin, S.J. Billinge, T. Vogt, and M. G. Kanatzidis: Structure of V_2O_5·nH_2O xerogel solved by the atomic pair distribution function technique. *J. Am. Chem. Soc.* **124**, 10157 (2002).
41. A. Moretti, F. Maroni, I. Osada, F. Nobili, and S. Passerini: V_2O_5 aerogel as a versatile cathode material for lithium and sodium batteries. *ChemElectroChem* **2**, 529 (2015).
42. Q. Wei, J. Liu, W. Feng, J. Sheng, X. Tian, L. He, Q. An, and L. Mai: Hydrated vanadium pentoxide with superior sodium storage capacity. *J. Mater. Chem. A* **3**, 8070 (2015).
43. Q. Wei, Z. Jiang, S. Tan, Q. Li, L. Huang, M. Yan, L. Zhou, Q. An, and L. Mai: Lattice breathing inhibited layered vanadium oxide ultrathin nanobelts for enhanced sodium storage. *ACS Appl. Mater. Inter.* **7**, 18211 (2015).
44. A. Moretti, S. Jeong, and S. Passerini: Enhanced cycling ability of V_2O_5 aerogel using room-temperature ionic liquid-based electrolytes. *Chem ElectroChem.* (2016). DOI: 10.1002/celc.201600040.
45. A. Moretti, M. Secchiaroli, D. Buchholz, G. Giuli, R. Marassi, and S. Passerini: Exploring the low voltage behavior of V_2O_5 aerogel as intercalation host for sodium ion battery. *J. Electrochem. Soc.* **14**, A2723 (2015).
46. X. Sun, C. Zhou, M. Xie, T. Hu, H. Sun, G. Xin, G. Wang, S.M. George, and J. Lian: Amorphous vanadium oxide coating on graphene by atomic layer deposition for stable high energy lithium ion anodes. *Chem. Commun.* **50**, 10703 (2014).
47. J. Sheng, Q. Li, Q. Wei, P. Zhang, Q. Wang, F. Lv, Q. An, W. Chen, and L. Mai: Metastable amorphous chromium-vanadium oxide nanoparticles with superior performance as a new lithium battery cathode. *Nano Res.* **7**, 1604 (2014).
48. O.B. Chae, J. Kim, I. Park, H. Jeong, J.H. Ku, J.H. Ryu, K. Kang, and S. M. Oh: Reversible lithium storage at highly populated vacant sites in an amorphous vanadium pentoxide electrode. *Chem. Mater.* **26**, 5874 (2014).
49. K. Salloux, F. Chaput, H. Wong, B. Dunn, and M. Breiter: Lithium intercalation in vanadium pentoxide aerogels. *J. Electrochem. Soc.* **142**, L191 (1995).
50. D. Le, S. Passerini, J. Guo, J. Ressler, B. Owens, and W. Smyrl: High surface area V_2O_5 aerogel intercalation electrodes. *J. Electrochem. Soc.* **143**, 2099 (1996).
51. D.R. Rolison and B. Dunn: Electrically conductive oxide aerogels: new materials in electrochemistry. *J. Mater. Chem.* **11**, 963 (2001).
52. E. Uchaker, Y. Zheng, S. Li, S. Candelaria, S. Hu, and G. Cao: Better than crystalline: amorphous vanadium oxide for sodium-ion batteries. *J. Mater. Chem. A* **2**, 18208 (2014).
53. S. Liu, Z. Tong, J. Zhao, X. Liu, J. Wang, X. Ma, C. Chi, Y. Yang, X. Liu, and Y. Li: Rational selection of amorphous or crystalline V_2O_5 cathode for sodium-ion batteries. *Phys. Chem. Chem. Phys.* **18**, 25645 (2016).
54. Z. Jian, C. Yuan, W. Han, X. Lu, L. Gu, X. Xi, Y.S. Hu, H. Li, W. Chen, and D. Chen: Atomic structure and kinetics of NASICON $Na_xV_2(PO_4)_3$ cathode for sodium-ion batteries. *Adv. Funct. Mater.* **24**, 4265 (2014).
55. K. Saravanan, C.W. Mason, A. Rudola, K.H. Wong, and P. Balaya: The first report on excellent cycling stability and superior rate capability of $Na_3V_2(PO_4)_3$ for sodium ion batteries. *Adv. Energy Mater.* **3**, 444 (2013).
56. Z. Jian, L. Zhao, H. Pan, Y.-S. Hu, H. Li, W. Chen, and L. Chen: Carbon coated $Na_3V_2(PO_4)_3$ as novel electrode material for sodium ion batteries. *Electrochem. Commun.* **14**, 86 (2012).
57. W. Shen, C. Wang, H. Liu, and W. Yang: Towards highly stable storage of sodium ions: a porous $Na_3V_2(PO_4)_3$/C cathode material for sodium-ion batteries. *Chem. – Eur. J.* **19**, 14712 (2013).
58. J. Liu, K. Tang, K. Song, P.A. van Aken, Y. Yu, and J. Maier: Electrospun $Na_3V_2(PO_4)_3$/C nanofibers as stable cathode materials for sodium-ion batteries. *Nanoscale* **6**, 5081 (2014).
59. W. Shen, H. Li, Z. Guo, C. Wang, Z. Li, Q. Xu, H. Liu, Y.G. Wang, and Y. Xia: Double nano-carbon synergistically modified $Na_3V_2(PO_4)_3$: an advanced cathode for high-rate and long life sodium-ion batteries. *ACS Appl. Mater. Interface* **8**, 24 (2016).
60. Y. Fang, L. Xiao, X. Ai, Y. Cao, and H. Yang: Hierarchical carbon framework wrapped Na_3V_2 $(PO_4)_3$ as a superior high-rate and extended lifespan cathode for sodium-ion batteries. *Adv. Mater.* **27**, 5895 (2015).
61. Y. Xu, Q. Wei, C. Xu, Q. Li, Q. An, P. Zhang, J. Sheng, L. Zhou, and L. Mai: Layer-by-layer $Na_3V_2(PO_4)_3$ embedded in reduced graphene oxide as superior rate and ultralong-life sodium-ion battery cathode. *Adv. Energy Mater.* **6**, 1600389 (2016).
62. W. Ren, Z. Zheng, C. Xu, C. Niu, Q. Wei, Q. An, K. Zhao, M. Yan, M. Qin, and L. Mai: Self-sacrificed synthesis of three-dimensional $Na_3V_2(PO_4)_3$ nanofiber network for high-rate sodium-ion full batteries. *Nano Energy* **25**, 145 (2016).
63. X. Wang, C. Niu, J. Meng, P. Hu, X. Xu, X. Wei, L. Zhou, K. Zhao, W. Luo, M. Yan, and L. Mai: Novel $K_3V_2(PO_4)_3$/C bundled nanowires as superior sodium-ion battery electrode with ultrahigh cycling stability. *Adv. Energy Mater.* **5**, 1500716 (2015).
64. X. Ma, W. Luo, M. Yan, L. He, and L. Mai: In situ characterization of electrochemical processes in one dimensional nanomaterials for energy storages devices. *Nano Energy* **24**, 165 (2016).
65. J. Wan, F. Shen, W. Luo, L. Zhou, J. Dai, X. Han, W. Bao, Y. Xu, J. Panagiotopoulos, and X. Fan: In situ transmission electron microscopy observation of sodiation-desodiation in a long cycle, high-capacity reduced graphene oxide sodium-ion battery anode. *Chem. Mater.* **28**, 6528 (2016).
66. X. Lu, E.R. Adkins, Y. He, L. Zhong, L. Luo, S.X. Mao, C.M. Wang, and B. A. Korgel: Germanium as a sodium ion battery material: in situ TEM reveals fast sodiation kinetics with high capacity. *Chem. Mater.* **28**, 1236 (2016).
67. C. Niu, X. Liu, J. Meng, L. Xu, M. Yan, X. Wang, G. Zhang, Z. Liu, X. Xu, and L. Mai: Three dimensional V_2O_5/NaV_6O_{15} hierarchical heterostructures: controlled synthesis and synergistic effect investigated by in situ X-ray diffraction. *Nano Energy* **27**, 147 (2016).
68. X.H. Liu, Y. Liu, A. Kushima, S. Zhang, T. Zhu, J. Li, and J.Y. Huang: In situ TEM experiments of electrochemical lithiation and delithiation of individual nanostructures. *Adv. Energy Mater.* **2**, 722 (2012).
69. M. Guignard, C. Didier, J. Darriet, P. Bordet, E. Elkaïm, and C. Delmas: P2-Na_xVO_2 system as electrodes for batteries and electron-correlated materials. *Nat. Mater.* **12**, 74 (2012).
70. Y. Wang and G. Cao: Synthesis and enhanced intercalation properties of nanostructured vanadium oxides. *Chem. Mater.* **18**, 2787 (2006).
71. R. Shakoor, D.H. Seo, H. Kim, Y.U. Park, J. Kim, S.W. Kim, H. Gwon, S. Lee, and K. Kang: A combined first principles and experimental study on $Na_3V_2(PO_4)_2F_3$ for rechargeable Na batteries. *J. Mater. Chem.* **22**, 20535 (2012).

72. K. Ogata, E. Salager, C. Kerr, A. Fraser, C. Ducati, A. Morris, S. Hofmann, and C.P. Grey: Revealing lithium–silicide phase transformations in nanostructured silicon-based lithium ion batteries via in situ NMR spectroscopy. *Nat. Commun.* **5**, 3217 (2014).
73. K.H. Wujcik, T.A. Pascal, C. Pemmaraju, D. Devaux, W.C. Stolte, N. P. Balsara, and D. Prendergast: Characterization of polysulfide radicals present in an ether-based electrolyte of a lithium–sulfur battery during initial discharge using in situ X-ray absorption spectroscopy experiments and first principles calculations. *Adv. Energy Mater.* **5**, 1500285 (2015).
74. F. Shi, P.N. Ross, H. Zhao, G. Liu, G.A. Somorjai, and K. Komvopoulos: A catalytic path for electrolyte reduction in lithium-ion cells revealed by in situ attenuated total reflection-fourier transform infrared spectroscopy. *J. Am. Chem. Soc.* **137**, 3181 (2015).
75. G. Venkatesh, V. Pralong, O. Lebedev, V. Caignaert, P. Bazin, and B. Raveau: Amorphous sodium vanadate $Na_{1.5+y}VO_3$, a promising matrix for reversible sodium intercalation. *Electrochem. Commun.* **40**, 100 (2014).
76. E. Uchaker and G. Cao: The role of intentionally introduced defects on electrode materials for alkali-ion batteries. *Chem. – Asian J.* **10**, 1608 (2015).
77. S. Komaba, T. Ishikawa, N. Yabuuchi, W. Murata, A. Ito, and Y. Ohsawa: Fluorinated ethylene carbonate as electrolyte additive for rechargeable Na batteries. *ACS Appl. Mater. Inter.* **3**, 4165 (2011).
78. Z. Hu, Z. Zhu, F. Cheng, K. Zhang, J. Wang, C. Chen, and J. Chen: Pyrite FeS_2 for high-rate and long-life rechargeable sodium batteries. *Energy Environ. Sci.* **8**, 1309 (2015).
79. A. Darwiche, C. Marino, M.T. Sougrati, B. Fraisse, L. Stievano, and L. Monconduit: Better cycling performances of bulk Sb in Na-ion batteries compared to Li-ion systems: an unexpected electrochemical mechanism. *J. Am. Chem. Soc.* **134**, 20805 (2012).
80. S. Yuan, X. Huang, D. Ma, H. Wang, F. Meng, and X. Zhang: Engraving copper foil to give large-scale binder-free porous CuO arrays for a high-performance sodium-ion battery anode. *Adv. Mater.* **26**, 2273 (2014).
81. M. Dahbi, T. Nakano, N. Yabuuchi, T. Ishikawa, K. Kubota, M. Fukunishi, S. Shibahara, J.Y. Son, Y.T. Cui, and H. Oji: Sodium carboxymethyl cellulose as a potential binder for hard-carbon negative electrodes in sodium-ion batteries. *Electrochem. Commun.* **44**, 66 (2014).